JOURNAL OF MATERIALS SCIENCE 8 (1973) 475–483

Planar defects in fibrous amphiboles

J. E. CHISHOLM*
Department of Geology, The University, Manchester, UK

The reciprocal lattice of the fibrous amphiboles is shown to consist of two sets of streaks or spikes, one parallel to x^*, the other to y^*. The first of these are interpreted in terms of stacking faults parallel to (100) with displacement $\pm \sim \frac{1}{3}\mathbf{c}$. The pyroxene, amphibole and talc structures are described as a family related by crystallographic shear operations and the streaks parallel to y^* ascribed to Wadsley defects parallel to (010).

1. Introduction

The amphibole group of minerals is chemically complex, having the general formula

$$AX_2Y_5Z_8O_{22}(OH, F)_2$$

where A = K, Na or vacancy, X = Na, Ca, Mg or Fe^{2+}, Y = Mg, Fe^{2+}, Fe^{3+} or Al, Z = Si or Al. The most important feature of the crystal structure of amphiboles is the linking of the $(Si, Al)O_4$ tetrahedra to form continuous double chains or bands parallel to the z-axis, with the octahedrally co-ordinated cations "sandwiched" between pairs of these bands [1].

The fibrous amphiboles are of considerable commercial importance in the asbestos industry which makes use of their unusual physical and chemical properties [2]. No previous attempt has been made to explore the microstructure of amphibole asbestos by electron microscopy and diffraction, earlier studies being concerned with the morphology of the fibres [3, 4].

2. Experimental

2.1. Material studied

The specimens of fibrous amphiboles used in this investigation are listed in Table I; all display the features and behaviour to be described.

TABLE I Fibrous amphiboles studied

	Approximate formula	Locality
Amosite	$Fe_{5.5}^{2+}Mg_{1.5}Si_8O_{22}(OH)_2$	Penge Weltevreden Dublin Mine
Crocidolite	$Na_2Fe_3^{2+}Fe_2^{3+}Si_8O_{22}(OH)_2$	Koegas Pomfret Wittenoom

2.2. Specimen preparation

A few small pieces of the fibre to be examined were ground under absolute alcohol for 5 to 10 min. One or two drops of the resulting suspension were transferred on to a thin vacuum-deposited carbon film on a specimen holder grid and the alcohol allowed to evaporate. The tiny crystals on the carbon support film were examined in an AEI EM6G electron microscope operating at 100 kV.

2.3. Morphology

The amphibole crystals observed in the electron microscope are on average about 1000 to 2000 Å wide and are distinctly elongated, their aspect ratio (length/width) ranging from about 3 to greater than 10. The electron diffraction patterns are consistent with the long direction of the crystals being parallel to the z-axis, which is the axis of the macroscopic fibres as determined optically and by X-ray diffraction.

3. Electron diffraction patterns

3.1. Indexing

In this discussion, indices will be given in terms of the monoclinic $C2/m$ unit cell [5].

The simplest type of diffraction pattern obtained from fibrous amphiboles is shown in Fig. 1 and consists of a rectangular mesh which can be indexed in terms of either of the two schemes of Fig. 2. The close similarity of the (001) and $(\bar{1}01)$ d-spacings and the variation of observed d^* values with specimen orientation prevent the two alternative sets of indices being distinguished.

*Present address: University of Sheffield, Department of Glass Technology, Northumberland Road, Sheffield.

Figure 1 Diffraction pattern; amosite, Penge mine. Note elongation of spots parallel to y^*.

3.2. Occurrence of extra reflections with $(h + k)$ odd

The C-face centred lattice leads one to expect reflections with $(h + k)$ odd to be systematically absent. Such reflections are, however, visible over the whole diffraction pattern whichever scheme of indexing is considered.

Reflections systematically absent because of lattice type can never occur as a result of double diffraction because such absences arise only from the choice of unit cell and not from any real feature of the structure. This conclusion can be confirmed by considering the conditions for double diffraction to occur [6]. It is then found that there are no pairs of reflections with $(h + k)$ even which can produce reflections with $(h + k)$ odd by double diffraction.

Amphiboles with space group $P2_1/m$ have been reported [7-10]. The possibility that the fibrous amphiboles may have this space group does not satisfactorily account for the extra reflections with $(h + k)$ odd for the following reasons.

(i) There are no signs of spots with $(h + k)$ odd on X-ray fibre photographs.

(ii) The amosite specimens for which chemical

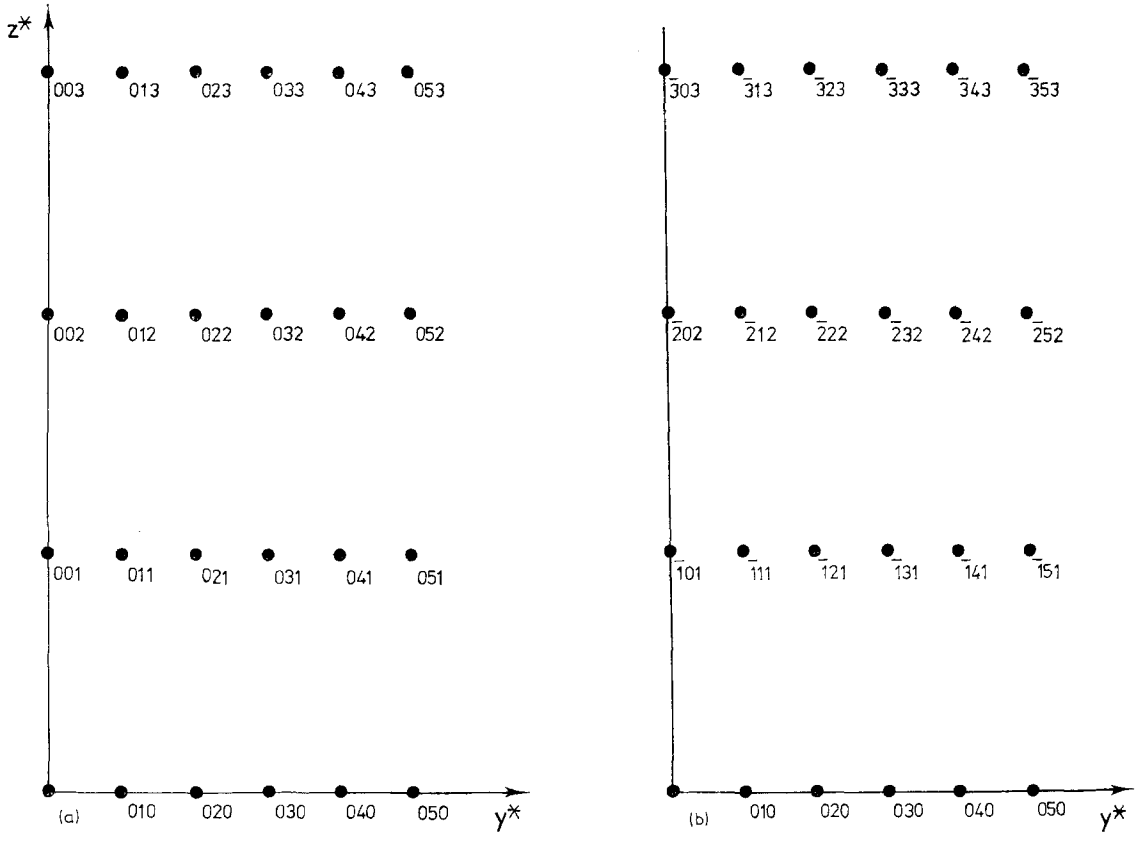

Figure 2 Possible schemes of indexing for the diffraction pattern of Fig. 1.

analyses are available [2] contain less than 2 wt% CaO which puts them outside the postulated composition range of the $P2_1/m$ structure [8].

(iii) Specimens in the electron beam reach a temperature of at least 200°C [11]. It is unlikely that the $P2_1/m$ structure could be observed in the electron microscope since the displacive transition from the $P2_1/m$ to the $C2/m$ structure probably occurs below 200°C. (For a cummingtonite a transition temperature as low as 40°C has been reported [12], but it is likely to vary considerably with composition.)

(iv) A primitive lattice will not explain the results of the tilting experiments described in the next section.

3.3. Streaks parallel to x^*

It is proposed that the fibrous amphiboles have a reciprocal lattice consisting of streaks or spikes parallel to x^* through the reciprocal lattice points. The intersection of these streaks with the reflecting sphere leads to the extra reflections apparently having indices with $(h + k)$ odd.

The only direct evidence for these streaks parallel to x^* so far obtained appears on the $(h0l)$ diffraction pattern of a crystal of grunerite (Fig. 3). In this non-fibrous specimen, the streaks are likely to be shorter and less intense than in the fibrous varieties [13].

The existence of the streaks parallel to x^* in the fibrous amphiboles can be inferred from indirect evidence and tilting experiments.

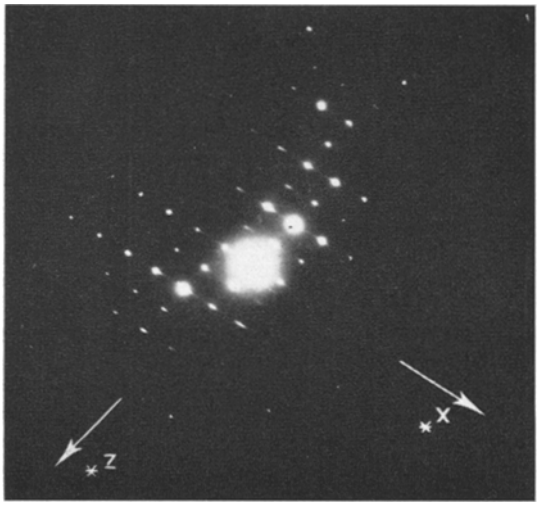

Figure 3 x^*-z^* diffraction pattern; grunerite, specimen no. 1 [14]. The streaks parallel to x^* are visible.

The values of b^* and of $d^*(001$ or $\bar{1}01)$ measured on diffraction patterns are often significantly larger than those expected from the cell parameters and camera constant. These variations are too large to be attributable to instrument operating conditions, specifically objective lens current, affecting the camera constant. At the same time, the observed b^* values are still closer to the expected d^* value of (010) than to that of any other reflection. The variations in observed b^* are attributed to the specimen being tilted, probably about the fibre axis (z), such that y^* is not perpendicular to the electron beam. The streaks parallel to x^* then intersect the plane perpendicular to the electron beam (which approximates to the surface of the reflecting sphere) at an angle such that the observed b^* is greater than the true value (Fig. 4). In a similar way, the variations in d^* (001 or $\bar{1}01$) are produced by the crystal being tilted about an axis approximately perpendicular to the fibre axis in such a way that the (001) or ($\bar{1}01$) reciprocal lattice vector is no longer perpendicular to the electron beam.

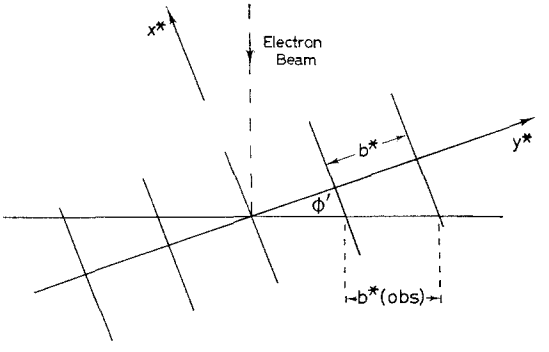

Figure 4 Geometry of tilting about z-axis. The plane perpendicular to the electron beam approximates to the surface of the reflecting sphere so that the observed b^* is always greater than the true value.

In order to check this interpretation and to confirm the existence of the streaks parallel to x^*, the effect of tilting the crystal on the diffraction pattern was examined using the Penge amosite specimen. The general appearance of the diffraction pattern changed very little even with 20 to 30° of tilt.

When a crystal is tilted about its long direction (fibre axis), the b^* repeat shows a systematic variation which is consistent with the geometry

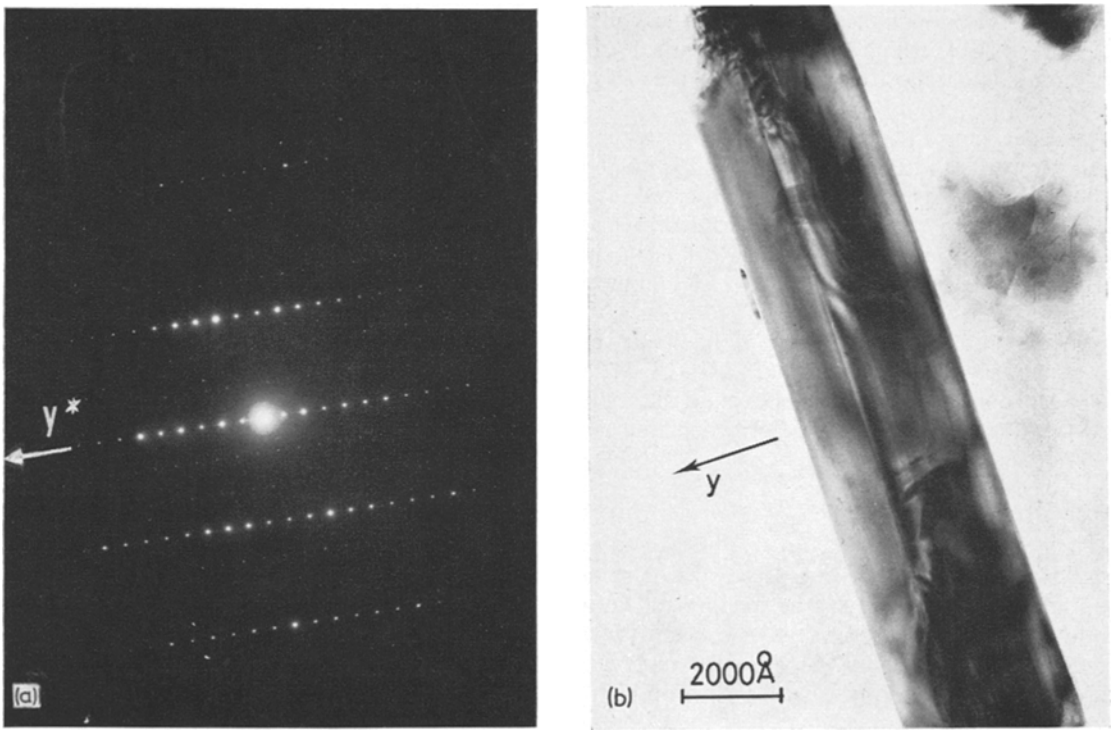

Figure 5 Amosite, Penge mine. (a) Diffraction pattern with intense streaks parallel to y^*. The intense reflections on the $l = 0$ and $l = \pm 3$ levels and the absence of some reflections on these levels are an effect of orientation of the crystal. (b) Micrograph showing Wadsley defects as diffuse lines of contrast perpendicular to y, i.e. parallel to the length of the crystal.

of tilting about the z-axis. No significant variation in d^* (001 or $\bar{1}01$) is found.

For tilting about an axis perpendicular to the fibre axis, d^* (001 or $\bar{1}01$) shows the systematic variation and there is no appreciable effect on b^*.

In addition, no sign of Laue zones is found on the diffraction patterns even in the tilting experiments. This further confirms the presence of streaks parallel to x^*.

3.4. Streaks parallel to y^*

The reciprocal lattice of the fibrous amphiboles also has streaks parallel to y^* through the reciprocal lattice points. These streaks are directly visible on the diffraction patterns (Figs. 1 and 5a). Their length and intensity, however, vary between crystals even in the same specimen because of differences either in orientation or in the number of defects. (Streaks parallel to y^* also occur in non-fibrous amphiboles but are less common than in the fibrous varieties [13].)

On X-ray fibre photographs, the streaks parallel to x^* and y^* appear as a faint diffuse distribution of intensity along the layer lines perpendicular to the z-axis.

4. Interpretation: planar defects

The starting point for the understanding of the streaks parallel to x^* and y^* is the theory of diffraction from structures containing stacking faults [15].

4.1. (100) stacking faults

The streaks parallel to x^* lie perpendicular to the plane of the stacking faults, (100).

The displacement vector of the stacking fault is determined in X-ray diffraction by noting which reflections have streaks and which have not. This method is not applicable to electron diffraction because dynamical interactions among the diffracted beams lead to streaks through all the reflections [16]. Nevertheless, from the known features of the amphibole structure it is possible to arrive at a plausible model for the (100) stacking faults.

The Si_4O_{11} double chains of the amphibole

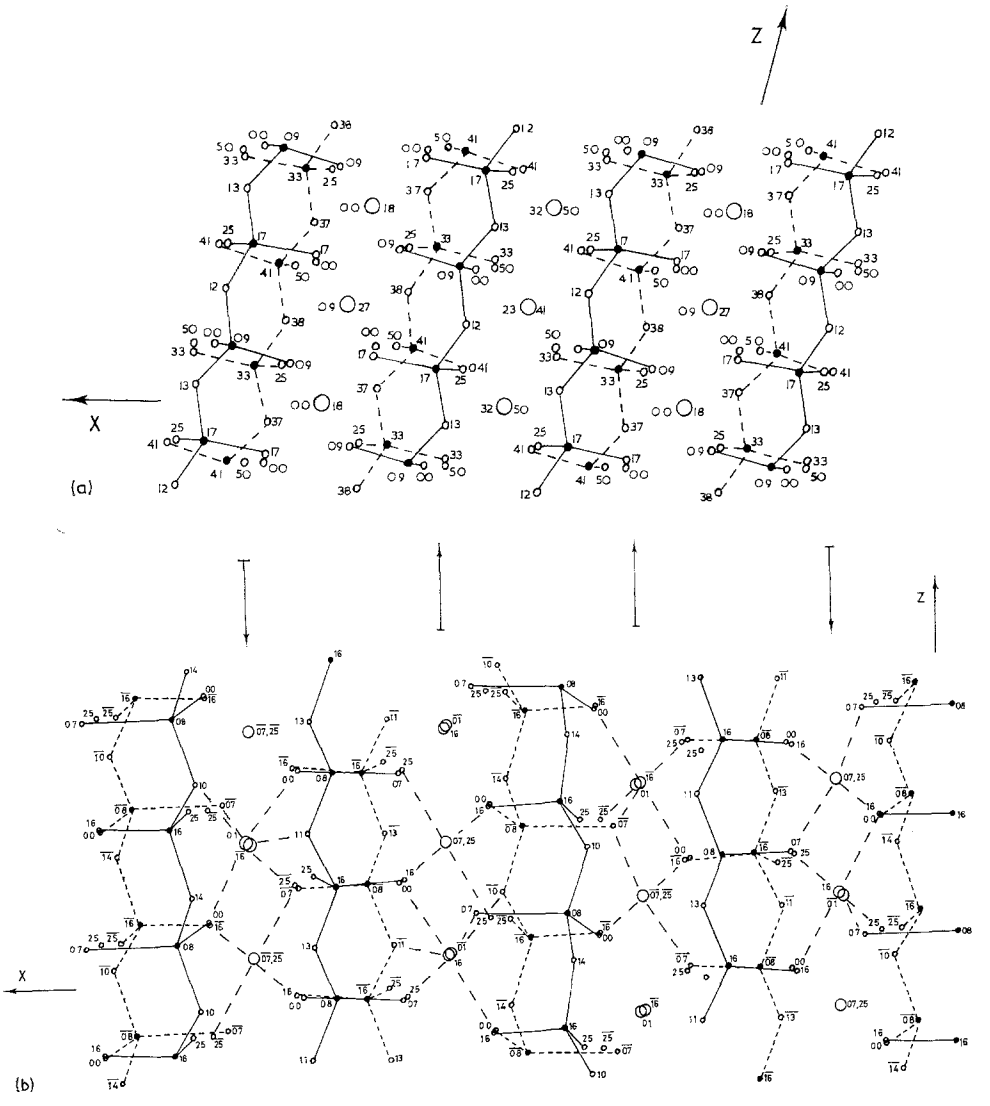

Figure 6 Projections of the amphibole structure on (010) with heights in units of $b/100$. (a) The monoclinic structure. Going along the $-x$ direction, successive tetrahedral layers are displaced by $-\sim\frac{1}{3}\mathbf{c}$. Based on the atomic co-ordinates of glauco-phane [21]. (b) The orthorhombic structure. Going along the $-x$ direction, the direction of displacement of the tetrahedral layers is shown by arrows at the top of the diagram. The co-ordination of the cations is shown by the coarser dashed lines and does not depend on the direction of displacement. Based on the atomic co-ordinates of gedrite 001 [22].

structure lie parallel to the (100) plane with layers of cations between them (Figs. 6a and b). Across each layer of cations, the two tetrahedral strips must be displaced by approximately $\pm\frac{1}{3}\mathbf{c}$ relative to each other in order to provide octahedral co-ordination for the cations. In the monoclinic amphiboles (Fig. 6a), these displacements are always in the same sense, giving the stacking sequence $+\,+\,+\,+\,+\,+\,\ldots$ or the alternative $-\,-\,-\,-\,-\,-\,\ldots$ related by the (100) twin law. The orthorhombic amphiboles (Fig. 6b) have the sequence $+\,+\,-\,-\,+\,+\,-\,-\,+\,\ldots$, corresponding to unit cell scale twinning of the monoclinic structure. The sequence $+\,-\,+\,-\,+\,-\,\ldots$ occurs in proto-amphibole [17], but this material also shows

the streaks parallel to x^* on Weissenberg photographs expected for faults in this stacking sequence.

In fibrous amphiboles, the streaks parallel to x^* result from mistakes in the regular $+\,+\,+\,+\,+\,+\,\ldots$ stacking sequence of the clino-amphibole structure. Two types of mistake are possible: (a) a (100) twin boundary, $\ldots\ +\,+\,+\,+\,-\,-\,-\,-\,\ldots$; (b) an isolated fault, $\ldots\ +\,+\,+\,+\,-\,+\,+\,+\,\ldots$.

No crystal has been obtained in an orientation suitable for deciding between these two alternatives.

4.2. (010) Wadsley defects

The streaks parallel to y^* are caused by faults on the (010) plane. Again a structurally reasonable model can be devised for these faults.

4.2.1. Crystallographic shear planes in the pyroxene, amphibole and talc structures

It is necessary to look at the crystal structures of pyroxene, amphibole and talc in the light of Wadsley's [18, 23] concept of crystallographic shear planes.

The clinopyroxene structure is shown schematically in Fig. 7a. It will be noted that going along the y-direction the chains "point" alternately towards $+x$ and $-x$, giving a stacking sequence $+\,-\,+\,-\,\ldots$. Consider a fault parallel to (010) in this structure (Fig. 7b) involving a displacement described as either $\frac{1}{2}\mathbf{a} + \frac{1}{2}\mathbf{c}$ or $\frac{1}{2}\mathbf{b} + \frac{1}{2}\mathbf{c}$, these two vectors being equivalent in the $C2/c$ structure. The atoms at such a fault will fit together satisfactorily if (i) the two chains share oxygen atoms, (ii) a single cation is placed on the fault plane midway between the unoccupied $M(2)$ positions of the two chains, (iii) two additional OH groups are inserted on the fault plane to provide octahedral co-ordination for the cation in (ii).

These requirements lead to an amphibole band in the neighbourhood of the (010) fault plane, with a stacking sequence $+\,-\,+\,-\,+\,+\,-\,+\,-$, but imply that this is not a simple stacking fault because of the change in composition.

Such a fault is most correctly described as a *crystallographic shear* (CS) *plane* [18, 23] since it displays all the features associated with such a defect:

(a) If the displacement is described as $\frac{1}{2}\mathbf{b} + \frac{1}{2}\mathbf{c}$, then it is not parallel to the fault plane.

(b) There is a closer linking of both the SiO_4 tetrahedra and the cation octahedra.

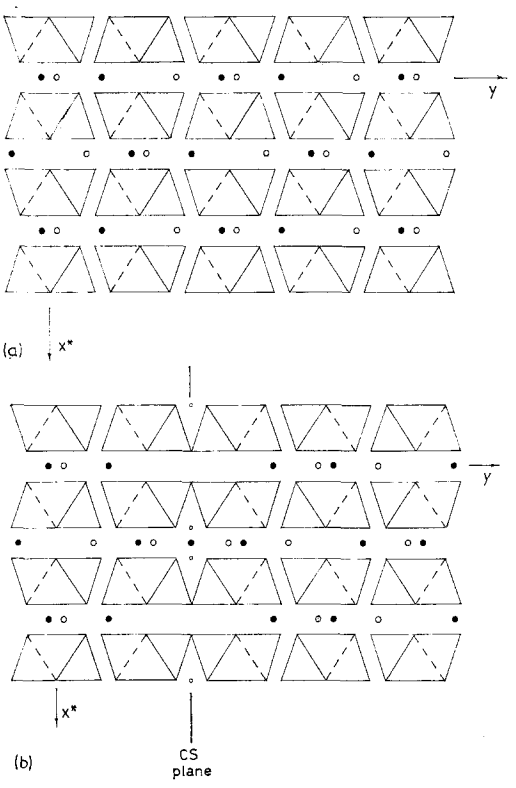

Figure 7 (a) Schematic drawing of the pyroxene structure viewed down the z-axis. The heights of the tetrahedra above the (001) plane are indicated by full and dashed lines. The cations are represented by large circles, their height being indicated by filled or open circles. (b) (010) CS plane in pyroxene. Small circles represent OH, height being shown by whether circle is open or filled.

(c) The fault has an associated departure from the ideal pyroxene composition.

A regular arrangement of such CS planes parallel to (010) at every second chain (Fig. 8a) corresponds in atomic arrangement and composition to the amphibole structure, with the chains having the sequence $+\,+\,-\,-\,+\,+\,-\,-\,\ldots$. If there is a CS plane at each chain, then the chains join together into the continuous sheets of the talc structure (Fig. 8b), with the sequence $+\,+\,+\,+\,+\,+\ldots$. along the y-direction.

This description of the pyroxene, amphibole and talc structures as a family related by crystallographic shear operations is a novel one and may have implications in crystal chemistry and mineralogy.

4.2.2. Wadsley defects

In structures with regular arrangements of CS

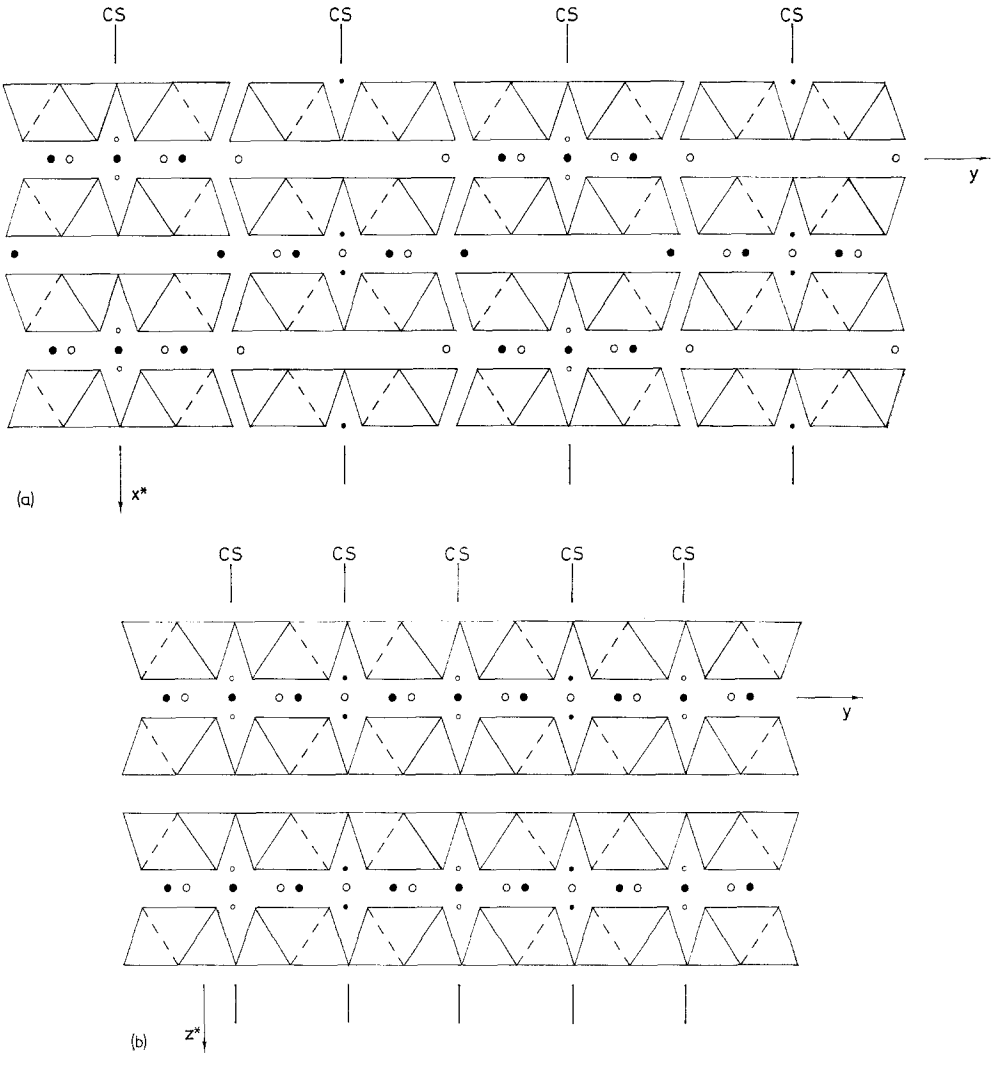

Figure 8 (a) The amphibole structure showing the CS planes. Heights shown are relative to the ($\bar{1}01$) plane of the $C2/m$ unit cell. (b) The talc structure showing CS planes. Same symbols as Fig. 7.

planes, mistakes sometimes occur in the regular sequence and are known as Wadsley defects [19]. In the amphibole structure such defects would be parallel to (010) and would lead to chain stacking sequences like

(I) . . . + + − − + + + − − + + . . . (Fig. 9a)

(II) . . . + + − − + − − + + . . . (Fig. 9b)

which respectively have "talc-like" and "pyrox-ene-like" regions at the defect. These two types of Wadsley defect involve departures from the ideal amphibole composition in opposite directions, i.e. if both types occur, their effect on bulk composition may be very small.

These Wadsley defects parallel to (010) are believed to be the cause of the streaks parallel to y^*. The defects are visible in electron micrographs (Fig. 5b) as diffuse lines of contrast parallel to the fibre axis. Their appearance is similar to that of Wadsley defects in a similar orientation described elsewhere [19, 20].

The spacing of these defects is variable but averages about 100 to 150Å. It can be shown that even if all the defects are of the same type, the departure from the ideal amphibole composition is no greater than that found in some chemical analyses [13].

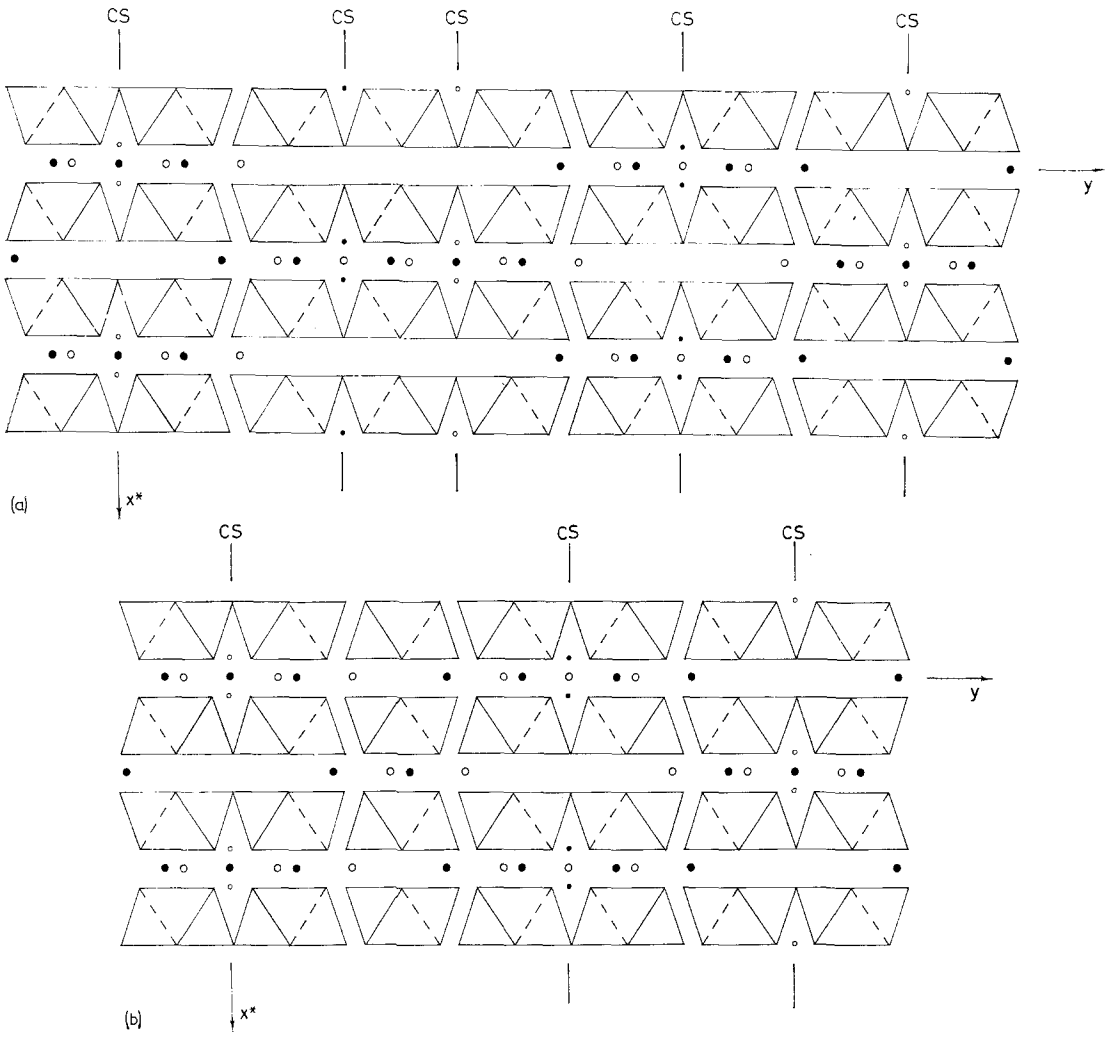

Figure 9 Wadsley defects in the amphibole structure, (a) type (I), (b) type (II) (see text). Same symbols as Fig. 7.

5. Conclusion

The presence of stacking faults parallel to (100) and Wadsley defects parallel to (010) in the fibrous amphiboles is likely to be important in relation to their mechanical properties and to the conditions and mechanism of their growth. It is hoped to explore these aspects further in the future.

Acknowledgements

The author is very grateful to Professor J. Zussman and Dr P. E. Champness for their helpful advice and criticism. Thanks are due to Cape Asbestos Fibres Ltd, Turner Brothers Asbestos Ltd, and Dr C. Klein Jun, for providing specimens. The electron microscope used in this investigation was provided for the Geology Department at Manchester University by a grant from the Natural Environment Research Council.

References

1. W. A. DEER, R. A. HOWIE, and J. ZUSSMAN, "Rock-forming Minerals", Vol. 2, Chain Silicates (Longmans, Green & Co, London, 1962).
2. A. A. HODGSON, "Fibrous Silicates" (Royal Institute of Chemistry, London, 1965).
3. M. S. BADOLLET, *Trans. Canad. Inst. Min. Metall.* **54** (1951) 151.
4. D. KING, *Trans. Roy. Soc. S. Aust.* **84** (1961) 119.
5. E. J. W. WHITTAKER and J. ZUSSMAN, *Acta Cryst.* **14** (1961) 54.

6. H. LIPSON and W. COCHRAN, "The Determination of Crystal Structures" (G. Bell & Sons, London, 1966).
7. M. G. BOWN, *Amer. Mineral.* **51** (1966) 259.
8. M. ROSS, J. J. PAPIKE, and P. W. WEIBLEN, *Science* **159** (1968) 1099.
9. H. J. KISCH, *Contr. Mineral. and Petrol.* **21** (1969) 319.
10. C. F. WOENSDREGT and P. HARTMAN, *Neues Jb. Mineral. Mh.* (1969) 558.
11. C. E. HALL, "Introduction to Electron Microscopy" (McGraw-Hill, London, 1966).
12. C. T. PREWITT, J. J. PAPIKE, and M. ROSS, *Earth Plan. Sci. Lett.* **8** (1970) 448.
13. J. E. CHISHOLM, Ph.D. Thesis, University of Manchester, 1972.
14. C. KLEIN, JUN, *Amer. Mineral.* **49** (1964) 963.
15. A. J. C. WILSON, "X-ray Optics" (Methuen, London, 1962).
16. P. B. HIRSCH, A. HOWIE, R. B. NICHOLSON, D. W. PASHLEY, and M. J. WHELAN, "Electron Microscopy of Thin Crystals" (Butterworths, London, 1965).
17. G. V. GIBBS, *Mineral. Soc. Amer. Spec. Pap.* **2** (1969) 101.
18. A. D. WADSLEY, "Reactivity of Solids", 6th Internat. Symp. (1968) 1.
19. J. G. ALLPRESS and J. V. SANDERS, "Electron Microscopy and Structure of Materials", Proc. 5th Internat. Materials Symp., 1971 (University of California Press, Berkeley, 1972), p. 134.
20. J. G. ALLPRESS, J. V. SANDERS, and A. D. WADSLEY, *Acta Cryst.* **B25** (1969) 1156.
21. J. J. PAPIKE and J. R. CLARK, *Amer. Mineral.* **53** (1968) 1156.
22. J. J. PAPIKE and M. ROSS, *ibid* **55** (1970) 1945.
23. J. S. ANDERSON, "Surface and Defect Properties of Solids", Vol. **1** (Chemical Society, London. 1972) p. 1.

Received 12 September and accepted 20 November 1972